Modeling of the Bias Temperature Instability Under Dynamic Stress and Recovery Conditions

T. Grasser[1*], B. Kaczer[2], H. Reisinger[3], P.-J. Wagner[1], and M. Toledano-Luque[2]

[1] Institute for Microelectronics, TU Wien, Austria [2] imec, Belgium [3] Infineon, Munich, Germany
[*] Email: grasser@iue.tuwien.ac.at

Abstract

The bias temperature instability (BTI) is one of the most important and controversial reliability issues in modern semiconductor devices. Recent modeling activities ascribe the phenomenon to the collective action of a large number of defects with widely distributed time constants. Using an analytic distribution of these time constants, highly-accurate closed-form expressions for BTI have been derived and recently extended to the high-frequency AC stress case. We review these latest efforts and demonstrate the validity of the model for a number of different technologies.

1. Introduction

Since devices in a circuit are not subjected to DC stress but to a time-dependent variation of the bias conditions, this fact has to be carefully considered in any modeling attempt. Compared to a conventional DC stress, AC stress patterns can significantly reduce the accumulated degradation [1–4]. While all studies report a duty-factor dependence following the ubiquitous step-shaped curve [1, 2, 5–8], the frequency dependence of BTI appears to be controversial: particularly older studies using slow measurements report frequency independent behavior [1, 9, 10], while more recent studies have revealed a frequency dependent contribution [3, 11–20]. We study the duty-factor and frequency dependence in the light of the recently proposed capture/emission time (CET) map model [7, 21–23] and demonstrate that the recoverable component of BTI can only to the first-order be captured by a two-state defect model. By using a three-state defect model, consistent with detailed studies on the microscopic defect properties [24, 25], the experimentally observed frequency dependence can be reproduced for a wide range of technologies.

2. Capture/Emission Time Map Model for BTI

It has recently been shown that both static as well as low-frequency dynamic BTI can be described by an ensemble of first-order defect reactions with a wide distribution of capture and emission times [21]. This model has been validated for various combinations of stress and recovery times for NBTI on SiON/pMOSFETs [7] and PBTI on high-k nMOSFETs [7, 22] both under static and dynamic

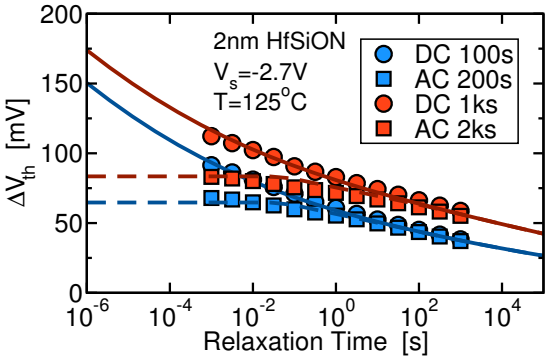

Fig. 1. Recovery after DC and AC stress for a nitrided HfSiON device at 125°C. As already demonstrated in [7, 22] for PBTI, recovery after AC stress of duration $2 \times t_s$ merges with the DC recovery after stress of duration t_s at $t_r = t_s$. The analytic model (solid lines for DC and dashed lines for AC) reproduces the data very well.

conditions. The wide distribution of time constants is visualized in the CET map, $g(\tau_c, \tau_e)$, as a function of the *effective* capture and emission times τ_c and τ_e. In a way, the CET map $g(\tau_c, \tau_e)$ contains the spectral information of the $\Delta V_{th}(t_s, t_r)$ curves, very much like in the Fourier transform theory [7].

Note, however, that the effective time constants in the CET map do not directly correspond to physical defect parameters like thermodynamic energy-levels or relaxation energies but are functions of them [25]. In this sense we wish to highlight that the CET map model *is not a new model meant to replace our previous modeling efforts* such as [24, 26]. Rather, the CET map model provides a convenient transformation of the experimental data to help understand the wide distribution of time constants [27].

We have recently suggested an analytic model for the CET map [23] using a recoverable (R) and a permanent (P) component, both of which are represented by bivariate normal distributions for the effective activation energies of the correlated capture and emission times. Given recent experimental evidence [21, 24, 28–31], all time constants are assumed to be thermally activated, $\tau = \tau_0 \exp(\beta E_A)$, with $\beta = 1/k_B T_L$, T_L the lattice temperature, and k_B the Boltzmann constant. Based on the analytic CET map, the overall degradation can be *analytically* calculated. Compact expressions for digital switching between two discrete gate bias levels have been given for any combination of

978-1-4673-2475-5/12/$31.00 ©2012 IEEE

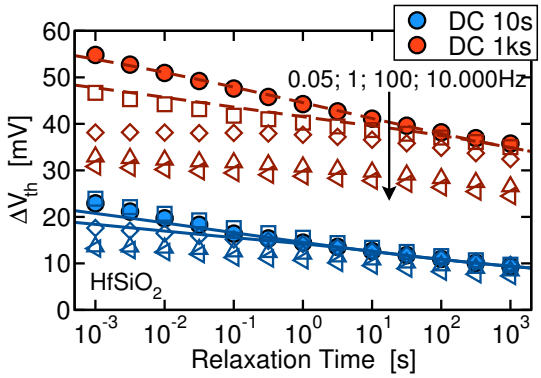

Fig. 2. While at 50 mHz the model (lines) agrees well with the data (syms), the model overestimates the degradation at higher frequencies, particularly in the non-nitrided sample shown above.

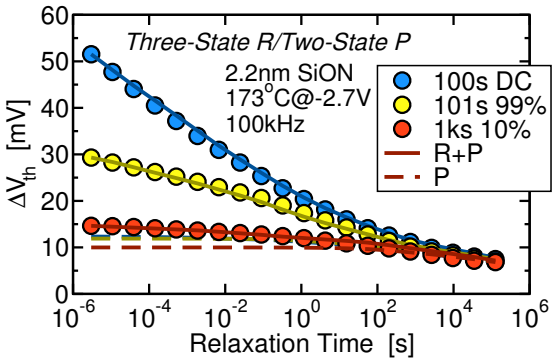

Fig. 3. The experimental recovery curves merge much later than predicted by the first-order model. By using frequency-dependent three-state defects for R, the experimental behavior can be well reproduced.

stress time/recovery time/duty factor, with excellent agreement to measurement data in the very wide window of stress and relaxation times from 1 μs to 100 ks [23]. While the accuracy of the model for DC and low-frequency AC stress is remarkable, see numerous comparisons in [23] and Fig. 1, discrepancies can be observed at higher frequencies.

3. Frequency dependence

Our discussion is based on the following simple prediction of the first-order model for an AC stress with duty-factor α and thus on/off ratio $\gamma = \alpha/(1-\alpha)$: Given that the duration of the AC stress equals t_s/α, with the cumulative stress time t_s, the build-up of slowly recoverable traps with $\tau_e > t_s/\gamma$ is the same under both conditions [7], *independent of frequency*. This is a simple consequence of the first-order reaction and completely independent of the actual distribution of the capture and emission times. Indeed, the merging of AC and DC recovery at the predicted recovery time has been experimentally confirmed for low-frequency AC PBTI on high-k [6, 7, 22] and low-frequency AC NBTI on SiO_2, SiON, HfSiO and HfSiON samples [23].

One possible explanation for the controversial reports on the frequency dependence is that during AC stress the degradation oscillates between the cumulative stress and recovery levels. Any fast measurement result will therefore critically depend on the measurement delay which, ideally, should be synchronized with the on/off stress condition. However, according to the first-order model [7, 22], any remnants of this frequency-dependent component will have recovered after $t_r = t_M$. As such, in order to remove this uncertainty, we propose to check for a frequency dependent contribution to BTI with a deliberately large delay at the merging point t_M. This would also be favorable from the perspective of reaction-diffusion-based theories which claim that the frequency-dependent hole-trapping component vanishes after a few seconds, leaving behind the frequency-independent RD contribution [8, 32].

We have experimentally tested the validity of the above first-order model prediction on a number of technologies (SiO_2, SiON, HfSiO, and HfSiON) and consistently found that **the predicted merging only occurs at low frequencies** ($< 1\,\text{Hz} - 100\,\text{Hz}$) [33]. In Fig. 2 it is demonstrated how the degradation level decreases with increasing frequency. The discrepancy is about 10% for the SiON device but can reach levels of 30% in the HfSiO device measured. This effect cannot be reproduced by the first-order model no matter what parameters are used, since it is a direct consequence of the underlying first-order reaction. We conclude that **either R or P (or both) cannot be described by a first-order reaction**. Given the known strong bias sensitivity of R [24, 34–36], we have recently concluded that P can be described by a first-order model while R requires a more detailed model [33].

4. Advanced CET Map Model

The CET map model is based on the assumption that the multi-state defect behavior observed previously [24] can be represented by an effective first-order (two-state) model. In particular, it was observed that the bias dependence of the effective capture time constant could be best explained by treating the change in the charge-state and the subsequent structural relaxation as a two-step process via an intermediate state 2′. The initial precursor state is given by 1 and the positive state is given by 2. Such a three-state model has also been used to explain the frequency dependence of PBTI in high-k pMOSFETs [16] under the assumption that the defects are negative-U centers.

Under DC conditions, the three-state defect can be approximated by a first-order (two-state) model using effective capture and emission time constants [25]. The approximation of a three-state defect by an effective two-state defect is valid provided the frequency does not become too large. For higher frequencies, the metastable state 2′ acts like a

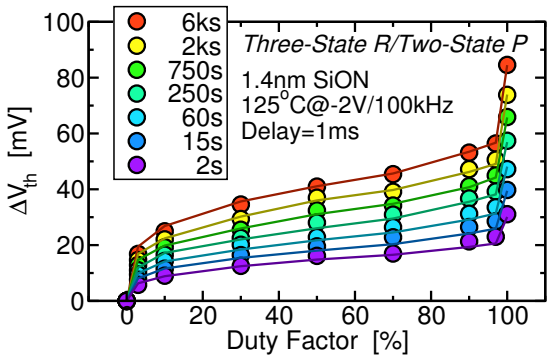

Fig. 4. Duty-factor dependent NBTI degradation (syms) as a function of increasing stress times measured with a delay of 1 ms. A frequency of 100 kHz was used. By using three-state defects for R, the duty-factor dependence can be accurately reproduced (lines). Note that the two-state model is not able to capture the strong impact of the AC stress [33].

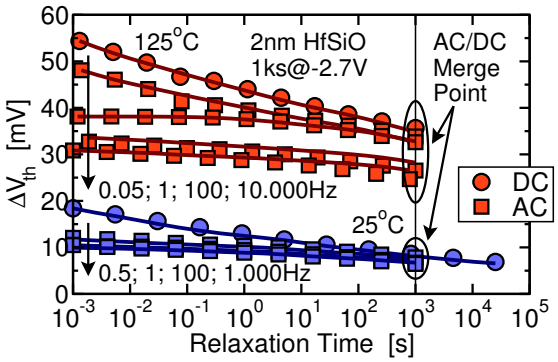

Fig. 5. Simulated (lines) vs. experimental (symbols) recovery after DC and AC stress for the HfSiO device at two temperatures. The merging point predicted by the simple first-order model is experimentally only observed at low frequencies. The discrepancy can be removed by assuming a three-state R component (lines).

low-pass filter while the transition from state $2'$ to 2 shows a *frequency-dependent effective capture time*.

As for low enough frequencies the three-state model simplifies to the two-state model, this implies that the predictions of the DC and low-frequency behavior are not affected by this extension of the model. As with the two-state model [7, 30], the response of the three-state defect to an AC signal can be evaluated in closed form, without the tedious requirement to resolve millions of cycles. While the derivation of the expressions is rather cumbersome compared to the elegant and simple solution of the two-state defect, they lead to a very simple results. In particular, the analytical formulas given previously [23] remain valid with suitable extensions, allowing for a very efficient analytic calculation of the AC degradation as a function of arbitrary stress and recovery times.

First, the model is evaluated on experimental data designed to reveal the merging point t_M using 3 different duty-factors, see Fig. 3. It has been observed previously [7] that the prediction of the two-state model is about 25% higher than the experimental data. In contrast, the three-state model can capture this effect correctly.

Second, although the two-state model can explain the qualitative features of the duty-factor dependence, comparison to experimental data remains unsatisfactory [7, 33]. In particular, it is impossible to introduce a large difference between $\alpha = 100\%$ (DC) and $\alpha = 50\%$ (AC) without significantly impacting the model accuracy for DC stress. As such, the simulated step is never as pronounced as that observed experimentally. Much better agreement is obtained with the three-state model as shown in Fig. 4. Remarkably, the ubiquitous shape of the curve is preserved even after a recovery time of 1 ks, including the peak at $\alpha = 100\%$. This is in stark contrast to RD theory papers [32], which claim that this peak is an artifact due to hole trapping and that the 'real' duty-factor dependence is given by RD theory. Quite to the contrary, given the preserved peak, we conclude again that hole trapping essentially determines NBTI even for longer stress and recovery times [8].

Third, the model is evaluated against the data recorded on the HfSiO device, which shows the strongest frequency dependence of 30% at 10 kHz. Again, while the two-state model shows no frequency dependence after a sufficiently long recovery period, the three-state model is consistent with the experimental data as shown in Fig. 5. In particular, even after a long recovery period, AC and DC data *do not merge*.

Finally, recent experimental evidence [37] demonstrates the very same frequency-dependence using individual traps in an extended time-dependent defect spectroscopy study [38], thereby confirming the fundamental assumption employed in this model.

5. Conclusions

We have studied the frequency dependence of BTI by using our previously developed capture/emission time map model, which is based on first-order reactions. While previous studies on the frequency dependence published in literature probably suffered from various issues – such as unspecified delay and a mixture of AC and recovery effects in the measured degradation level – our study deliberately uses long recovery times equal to the theoretical first-order AC/DC merging point. The observed deviation from the first-order model means that defect charging follows first-order kinetics only in the low-frequency limit. Consistent with the previously described switching traps, introduction of a third defect state provides a good description of the experimentally observed frequency dependence for a number of different technologies.

6. Acknowledgments

The research leading to these results has received funding from the FWF project n°23390-M24 and the European Community's FP7 project n°261868 (MORDRED).

References

[1] R. Fernández, B. Kaczer, A. Nackaerts, S. Demuynck, R. Rodriguez, M. Nafria, and G. Groeseneken, "AC NBTI Studied in the 1 Hz - 2 GHz Range on Dedicated On-Chip CMOS Circuits," in *Proc. Intl.Electron Devices Meeting (IEDM)*, 2006, pp. 337–340.

[2] T. Grasser, B. Kaczer, P. Hehenberger, W. Goes, R. O'Connor, H. Reisinger, W. Gustin, and C. Schlünder, "Simultaneous Extraction of Recoverable and Permanent Components Contributing to Bias-Temperature Instability," in *Proc. Intl.Electron Devices Meeting (IEDM)*, 2007, pp. 801–804.

[3] T. Nigam, "Pulse-Stress Dependence of NBTI Degradation and Its Impact on Circuits," *IEEE Trans.Dev.Mat.Rel.*, vol. 8, no. 1, pp. 72–78, 2008.

[4] Z. Teo, A. Boo, D. Ang, and K. Leong, "On the Cyclic Threshold Voltage Shift of Dynamic Negative-Bias Temperature Instability," in *Proc. Intl.Rel.Phys.Symp. (IRPS)*, 2011, pp. 943–947.

[5] B. Kaczer, T. Grasser, P. Roussel, J. Martin-Martinez, R. O'Connor, B. O'Sullivan, and G. Groeseneken, "Ubiquitous Relaxation in BTI Stressing-New Evaluation and Insights," in *Proc. Intl.Rel.Phys.Symp. (IRPS)*, 2008, pp. 20–27.

[6] K. Zhao, J. Stathis, A. Kerber, and E. Cartier, "PBTI Relaxation Dynamics after AC vs. DC Stress in High-k/Metal Gate Stacks," in *Proc. Intl.Rel.Phys.Symp. (IRPS)*, Apr. 2010, pp. 50–54.

[7] H. Reisinger, T. Grasser, K. Ermisch, H. Nielen, W. Gustin, and C. Schlünder, "Understanding and Modeling AC BTI," in *Proc. Intl.Rel.Phys.Symp. (IRPS)*, Apr. 2011, pp. 597–604.

[8] T. Grasser, B. Kaczer, W. Goes, H. Reisinger, T. Aichinger, P. Hehenberger, P.-J. Wagner, F. Schanovsky, J. Franco, M. Toledano-Luque, and M. Nelhiebel, "The Paradigm Shift in Understanding the Bias Temperature Instability: From Reaction-Diffusion to Switching Oxide Traps," *IEEE Trans.Electron Devices*, vol. 58, no. 11, pp. 3652–3666, 2011.

[9] G. Chen, M. Li, C. Ang, J. Zheng, and D. Kwong, "Dynamic NBTI of p-MOS Transistors and its Impact on MOSFET Scaling," *IEEE Electron Device Lett.*, vol. 23, no. 12, pp. 734 – 736, dec 2002.

[10] M. Alam, "A Critical Examination of the Mechanics of Dynamic NBTI for pMOSFETs," in *Proc. Intl.Electron Devices Meeting (IEDM)*, 2003, pp. 345–348.

[11] W. Abadeer and W. Ellis, "Behavior of NBTI under AC Dynamic Circuit Conditions," in *Proc. Intl.Rel.Phys.Symp. (IRPS)*, 2003, pp. 17–22.

[12] V. Huard, M. Denais, F. Perrier, and C. Parthasarathy, "Static and Dynamic NBTI Stress in pMOS Transistors," in *Proc. Insulating Films Semicond. (INFOS)*, 2003, pp. 1–2.

[13] S. Chakravarthi, A. Krishnan, V. Reddy, C. Machala, and S. Krishnan, "A Comprehensive Framework for Predictive Modeling of Negative Bias Temperature Instability," in *Proc. Intl.Rel.Phys.Symp. (IRPS)*, 2004, pp. 273–282.

[14] S. Mahapatra, M. Alam, P. Kumar, T. Dalei, and D. Saha, "Mechanism of Negative Bias Temperature Instability in CMOS Devices: Degradation, Recovery and Impact of Nitrogen," in *Proc. Intl.Electron Devices Meeting (IEDM)*, 2004, pp. 105–108.

[15] V. Huard, M. Denais, F. Perrier, N. Revil, C. Parthasarathy, A. Bravaix, and E. Vincent, "A Thorough Investigation of MOSFETs NBTI Degradation," *Microelectronics Reliability*, vol. 45, no. 1, pp. 83–98, 2005.

[16] C. Shen, M. Li, H. Yu, X. Wang, Y.-C. Yeo, D. Chan, and D.-L. Kwong, "Physical Model for Frequency-Dependent Dynamic Charge Trapping in Metaloxide-Semiconductor Field Effect Transistors with HfO_2 Gate Dielectric," *Appl.Phys.Lett.*, vol. 86, p. 093510, 2005.

[17] A. Krishnan, C. Chancellor, S. Chakravarthi, P. Nicollian, V. Reddy, A. Varghese, R. Khamankar, and S. Krishnan, "Material Dependence of Hydrogen Diffusion: Implications for NBTI Degradation," in *Proc. Intl.Electron Devices Meeting (IEDM)*, 2005, pp. 688–691.

[18] S. Zhu, A. Nakajima, T. Ohashi, and H. Miyake, "Interface Trap Generation Induced by Charge Pumping Current Under Dynamic Oxide Field Stresses," *IEEE Electron Device Lett.*, vol. 26, no. 3, pp. 216–219, 2005.

[19] Y. Mitani, H. Satake, and A. Toriumi, "Influence of Nitrogen on Negative Bias Temperature Instability in Ultrathin SiON," *IEEE Trans.Dev.Mat.Rel.*, vol. 8, no. 1, pp. 6–13, 2008.

[20] S. Wang, D. Ang, and G. Du, "Effect of Nitrogen on the Frequency Dependence of Dynamic NBTI-Induced Threshold-Voltage Shift of the Ultrathin Oxynitride Gate P-MOSFET," *IEEE Electron Device Lett.*, vol. 29, no. 5, pp. 483–486, 2008.

[21] H. Reisinger, T. Grasser, W. Gustin, and C. Schlünder, "The Statistical Analysis of Individual Defects Constituting NBTI and its Implications for Modeling DC- and AC-Stress," in *Proc. Intl.Rel.Phys.Symp. (IRPS)*, May 2010, pp. 7–15.

[22] K. Zhao, J. Stathis, B. Linder, E. Cartier, and A. Kerber, "PBTI Under Dynamic Stress: From a Single Defect Point of View," in *Proc. Intl.Rel.Phys.Symp. (IRPS)*, Apr. 2011, pp. 372–380.

[23] T. Grasser, P.-J. Wagner, H. Reisinger, T. Aichinger, G. Pobegen, M. Nelhiebel, and B. Kaczer, "Analytic Modeling of the Bias Temperature Instability Using Capture/Emission Time Maps," in *Proc. Intl.Electron Devices Meeting (IEDM)*, Dec. 2011, pp. 27.4.1–27.4.4.

[24] T. Grasser, H. Reisinger, P.-J. Wagner, W. Goes, F. Schanovsky, and B. Kaczer, "The Time Dependent Defect Spectroscopy (TDDS) for the Characterization of the Bias Temperature Instability," in *Proc. Intl.Rel.Phys.Symp. (IRPS)*, May 2010, pp. 16–25.

[25] T. Grasser, "Stochastic Charge Trapping in Oxides: From Random Telegraph Noise to Bias Temperature Instabilities," in *Microelectronics Reliability*, vol. 52, 2012, pp. 39–70.

[26] T. Grasser, B. Kaczer, W. Goes, T. Aichinger, P. Hehenberger, and M. Nelhiebel, "A Two-Stage Model for Negative Bias Temperature Instability," in *Proc. Intl.Rel.Phys.Symp. (IRPS)*, 2009, pp. 33–44.

[27] B. Kaczer, T. Grasser, J. Martin-Martinez, E. Simoen, M. Aoulaiche, P. Roussel, and G. Groeseneken, "NBTI from the Perspective of Defect States with Widely Distributed Time Scales," in *Proc. Intl.Rel.Phys.Symp. (IRPS)*, 2009, pp. 55–60.

[28] T. Aichinger, M. Nelhiebel, and T. Grasser, "On the Temperature Dependence of NBTI Recovery," *Microelectronics Reliability*, vol. 48, no. 3, pp. 1178–1184, 2008.

[29] M. Toledano-Luque, B. Kaczer, E. Simoen, P. Roussel, A. Veloso, T. Grasser, and G. Groeseneken, "Temperature and Voltage Dependences of the Capture and Emission Times of Individual Traps in High-κ Dielectrics," in *Proc. Insulating Films Semicond. (INFOS)*, 2011.

[30] M. Toledano-Luque, B. Kaczer, P. J. Roussel, M. Cho, T. Grasser, and G. Groeseneken, "Temperature Dependence of the Emission and Capture Times of SiON Individual Traps after Positive Bias Temperature Stress," *J.Vac.Sci.Technol.B*, vol. 29, pp. 01AA04–1–01AA04–5, 2011.

[31] M. Toledano-Luque, B. Kaczer, E. Simoen, P. J. Roussel, A. Veloso, T. Grasser, and G. Groeseneken, "Temperature and Voltage Dependences of the Capture and Emission Times of Individual Traps in High-k Dielectrics," *Microelectronic Engineering*, vol. 88, pp. 1243–1246, 2011.

[32] A. Islam, S. Mahapatra, S. Deora, V. Maheta, and M. Alam, "Essential Aspects of Negative Bias Temperature Instability (NBTI)," http://www.nanohub.org, 2011.

[33] T. Grasser, B. Kaczer, H. Reisinger, P.-J. Wagner, and M. Toledano-Luque, "On the Frequency Dependence of the Bias Temperature Instability," in *Proc. Intl.Rel.Phys.Symp. (IRPS)*, Apr. 2012, pp. XT.8.1–XT.8.7.

[34] T. Grasser, B. Kaczer, and W. Goes, "An Energy-Level Perspective of Bias Temperature Instability," in *Proc. Intl.Rel.Phys.Symp. (IRPS)*, 2008, pp. 28–38.

[35] T. Aichinger, M. Nelhiebel, and T. Grasser, "Unambiguous Identification of the NBTI Recovery Mechanism using Ultra-Fast Temperature Changes," in *Proc. Intl.Rel.Phys.Symp. (IRPS)*, 2009, pp. 2–7.

[36] T. Grasser, T. Aichinger, G. Pobegen, H. Reisinger, P.-J. Wagner, J. Franco, M. Nelhiebel, and B. Kaczer, "The 'Permanent' Component of NBTI: Composition and Annealing," in *Proc. Intl.Rel.Phys.Symp. (IRPS)*, Apr. 2011, pp. 605–613.

[37] T. Grasser, H. Reisinger, K. Rott, M. Toledano-Luque, and B. Kaczer, "On the Microscopic Origin of the Frequency Dependence of Hole Trapping in pMOSFETs," in *Proc. Intl.Electron Devices Meeting (IEDM)*, Dec. 2012, (in print).

[38] T. Grasser, H. Reisinger, P.-J. Wagner, and B. Kaczer, "The Time Dependent Defect Spectroscopy for the Characterization of Border Traps in Metal-Oxide-Semiconductor Transistors," *Physical Review B*, vol. 82, no. 24, p. 245318, 2010.